

Gapped Spin Excitation in Magnetic Ordered State on Yb-Based Zigzag Chain Compound YbAgSe₂

Fumiya Hori^{1*}, Shunsaku Kitagawa¹, Kenji Ishida¹,
Souichiro Mizutani², Yudai Ohmagari² and Takahiro Onimaru²

¹*Department of Physics, Kyoto University, Kyoto 606-8502, Japan*

²*Department of Quantum Matter, Graduate School of Advanced Science and Engineering, Hiroshima University, Higashihiroshima 739-8530, Japan*

We report the ⁷⁷Se-nuclear magnetic resonance (NMR) results of trivalent Yb zigzag chain compound YbAgSe₂, which is a sister compound of YbCuS₂. The ⁷⁷Se-NMR spectrum was reproduced by considering two different Se sites with negative Knight shifts and three-axis anisotropy. Above the Néel temperature T_N , the Knight shift is proportional to the bulk magnetic susceptibility. Below T_N , the extremely broad signal with weak intensity and the relatively sharp signal coexist, suggesting that one is strongly influenced by internal magnetic fields and the other remains relatively unaffected by these fields in the magnetic ordered state. The nuclear spin-lattice relaxation rate $1/T_1$ remains almost constant above T_N and abruptly decreases below T_N . In contrast to YbCuS₂, a T -linear behavior of $1/T_1$ at low temperatures was not observed at least down to 1.0 K in YbAgSe₂. Our results indicate that the gapless excitation is unique to YbCuS₂, or is immediately suppressed in the magnetic fields.

1. Introduction

In recent years, there has been significant attention and interest in novel charge-neutral quasiparticles observed in strongly correlated insulators.¹⁻¹²⁾ The gapless excitations of such quasiparticles, which are seemingly inconsistent with the bulk charge-band gap observed in transport measurements, have been reported in some rare-earth based compounds; Yb-based frustrated insulating magnets YbMgGaO₄¹⁻³⁾ and NaYbSe₂,^{4,5)} Kondo insulators YbB₁₂⁶⁻⁸⁾ and YbIr₃Si₇.^{9,10)} YbCuS₂ is one of such rare-earth-based compounds, where the Yb³⁺ ions with magnetic moments form zigzag chains along the a axis.¹³⁾ Due to the competing interactions between nearest and next-nearest neighbors in the zigzag chains, magnetic frustration is expected in YbCuS₂.¹⁴⁻²⁰⁾ At zero magnetic field, the specific heat exhibits a sharp peak at $T_N \sim 0.95$ K.^{21,22)} In the previous study,¹²⁾ we performed ^{63/65}Cu-nuclear quadrupole resonance (NQR) measurements and revealed the first-order magnetic transition at T_N and an incommensurate magnetic structure with much smaller Yb magnetic moments than the anticipated one from the crystalline electric field ground state. In addition, we found the gapless excitations in YbCuS₂, suggesting the presence of the charge-neutral quasiparticles. Although the magnetic frustration arising from the Yb zigzag chains seems to play a crucial role in leading to this ordered state and the gapless excitations,^{11,12)} the origin and the characteristics of these phenomena still remain unclear. Recently, it has been theoretically proposed that the anisotropic exchange interactions originating from the Yb zigzag chains may lead to gapless excitations.¹⁸⁻²⁰⁾ Therefore, the investigation on other Yb-based zigzag-chain compounds

is highly desired.

Yb-based compound YbAgSe₂ has an orthorhombic structure with the space group $P2_12_12_1$ (No. 19, D_2^4) and the Yb zigzag chains are formed as shown in Fig. 1(a),²³⁾ similar to YbCuS₂.¹³⁾ There are two crystallographically different Se sites. The value of the effective magnetic moment estimated from the magnetic susceptibility above 40 K is $4.77 \mu_B$, which is close to that expected for the trivalent Yb³⁺ ions ($4.54 \mu_B$).²⁴⁾ The Weiss temperature estimated from the simple Curie-Weiss fitting of the magnetic susceptibility below 300 K is -71.9 K, indicating the predominance of the antiferromagnetic interactions, similar to YbCuS₂. Although the magnetic specific heat exhibits a lambda-type anomaly at the magnetic transition temperature $T_N \sim 1.8$ K, the magnetic entropy at T_N is only 30% of $R \ln 2$ expected for the crystalline electric field ground-state doublet, indicating the presence of the magnetic fluctuations above T_N .²⁴⁾ As T_N is much smaller than the Weiss temperature and a peculiar temperature-magnetic field phase diagram similar to that observed in YbCuS₂ was obtained,²⁵⁾ magnetic frustration due to the Yb zigzag chains is expected.

In this paper, we report the magnetic ordered state and low-energy magnetic excitations investigated from microscopic point of view with the ⁷⁷Se-nuclear magnetic resonance (NMR). Below T_N , the NMR spectral intensity suddenly decreases, and the sharp and broad signals were observed. This indicates that the internal magnetic fields at the two crystallographically distinct sites below T_N are different from each other. The nuclear spin-lattice relaxation rate $1/T_1$ stays almost constant above T_N and suddenly decreases below T_N , suggesting a gapped magnetic ordered state. T -linear behavior observed in YbCuS₂ was not detected down to 1.0 K

*hori.fumiya.36s@st.kyoto-u.ac.jp

in YbAgSe₂.

2. Experimental

Polycrystalline samples of YbAgSe₂ were synthesized by melting the constituent elements in evacuated quartz ampoules.²⁴⁾ A conventional spin-echo technique was used for the ⁷⁷Se-NMR measurements. ⁷⁷Se nucleus, the natural abundance of which is 7.6 %, has nuclear spin $I = 1/2$ with nuclear gyromagnetic ratio of ${}^{77}\gamma/2\pi = 8.12$ MHz/T. A ³He-⁴He dilution refrigerator was used for the NMR measurement below 1.4 K. The ⁷⁷Se-NMR spectra were obtained by the H -swept measurement. The Knight shift K was measured at fixed frequencies of 24.4 (~ 3 T) and 84.12 MHz (~ 11 T). Since it is difficult to separate the signals arising from the two sites in the spectrum measured at 24.4 MHz, the average value of Knight shift K_{av} was estimated from the first moment of the NMR spectrum. The nuclear spin-lattice relaxation rate $1/T_1$ was evaluated by fitting the relaxation curve of the nuclear magnetization after its saturation to a theoretical function for the nuclear spin $I = 1/2$, which is a single exponential function on the polycrystalline sample. $1/T_1$ was measured at 3 T (22.4 MHz) above 1.5 K and 1 T (9.35 MHz) below 3 K.

3. Results and Discussion

Figure 1(b) shows the ⁷⁷Se-NMR spectrum obtained by H -swept method at the frequencies of $f = 24.4$ MHz and 84.12 MHz at 4.2 K on the powdered YbAgSe₂, where the horizontal axis is $K = (2\pi f/\gamma - H)/H$. While the spectrum measured at a higher frequency has a higher resolution, NMR spectra at both frequencies are nearly identical and H -independent. Since YbAgSe₂ has two different Se sites as shown in the Fig. 1(a),²³⁾ two ⁷⁷Se-NMR signals are considered to overlap with each other. The NMR spectrum was well fitted by the simulation assuming the two different Se sites with negative Knight shifts and three-axis anisotropy $(K_x^1, K_y^1, K_z^1) = -(2.2, 6.0, 8.0)\%$ and $(K_x^2, K_y^2, K_z^2) = -(2.2, 4.8, 10.3)\%$, respectively. Here, K_i^j is i -axis Knight shift at the Se site j ($i = x, y, z, j = 1, 2$). As the values of K_i^1 and K_i^2 are close to each other, the site assignment is difficult in the present NMR measurements.

As shown in Fig. 2(a), the NMR spectrum becomes broader and shifts toward the higher magnetic fields above T_N with decreasing temperature. Figure 2(b) exhibits the temperature dependence of K_{av} measured at 24.4 MHz. Above T_N , the absolute value of K_{av} increases with decreasing temperature, and follows the Curie-Weiss behavior. K_{av} is scaled with the bulk magnetic susceptibility χ . From the $K_{\text{av}}\text{-}\chi$ plot with χ measured at 0.1 T,²⁴⁾ the hyperfine coupling constant A_{hf} was estimated to be -0.47 T/ μ_B as shown in Fig. 2(c). Here, the hyperfine coupling constant is the proportionality constant for the Knight shift with respect to magnetic susceptibility, and thus can be obtained from the slope of the $K\text{-}\chi$ plot. Such a negative hyperfine coupling constant was often observed in several Yb-based systems.²⁶⁻³⁰⁾ Below $T_N \sim 1.8$ K, the spectral intensity decreases. It seems that one of the NMR spectra becomes broadened below T_N , the signal intensity of which

is too weak to be observed in the whole region [black dashed curve of Fig. 2(a)], and that the relatively sharp peak signal remains [black solid curve of Fig. 2(a)]. Therefore, the internal magnetic fields at the two crystallographically distinct sites below T_N are different from each other: one site is strongly affected by the internal magnetic fields and the other is not. Determining which Se site is more strongly affected by the internal magnetic fields requires information about the magnetic structure. Thus, in order to determine the magnetic structure, the neutron scattering measurements are necessary.

Main figure of Fig. 3 shows the nuclear spin-lattice relaxation rate $1/T_1$ measured at the peak of the ⁷⁷Se-NMR spectrum on YbAgSe₂. $1/T_1$ remains almost constant above T_N , which is usually observed in localized spin systems. Below T_N , $1/T_1$ decreases more rapidly than T^5 dependence. Tentatively, when the observed sharp decrease in $1/T_1$ down to 1.0 K is fitted to a thermally activated behavior $1/T_1 \sim \exp(-\Delta/T)$ with a magnon gap Δ , it is obtained as $\Delta \sim 9$ K, which is larger than the transition temperature T_N .

Here, we discuss the hyperfine coupling constant and low-energy excitations of YbAgSe₂ in comparison with those of YbCuS₂. The absolute value of $A_{\text{hf}} = -0.47$ T/ μ_B in YbAgSe₂, determined from the slope of the $K\text{-}\chi$ plot, is three times larger than 0.14 T/ μ_B in YbCuS₂.³²⁾ In general, hyperfine coupling constant in insulators or semiconductors originates from the classical dipolar interaction. However, A_{hf} evaluated in YbAgSe₂ is much larger than the hyperfine coupling constant estimated from the classical dipolar interaction A_d , which is given by

$$A_d = \sum_i 9.2741 \times 10^{-1} \times \frac{1}{r_i^5} \begin{pmatrix} 3x_i^2 - r_i^2 & 3x_i y_i & 3x_i z_i \\ 3y_i x_i & 3y_i^2 - r_i^2 & 3y_i z_i \\ 3z_i x_i & 3z_i y_i & 3z_i^2 - r_i^2 \end{pmatrix} \quad (\text{T}/\mu_B), \quad (1)$$

where r_i (\AA) is a distance between Se and Yb- i sites. From the eq. (1),

$$A_d^{\text{Se}(1)} = \begin{pmatrix} 0.0046 & -0.0027 & 0.0051 \\ -0.0027 & 0.0018 & 0.0082 \\ 0.0051 & 0.0082 & -0.0064 \end{pmatrix} \quad (\text{T}/\mu_B) \quad (2)$$

for the Se(1) site, and

$$A_d^{\text{Se}(2)} = \begin{pmatrix} 0.0078 & 0.0029 & -0.0030 \\ 0.0029 & -0.0097 & -0.1023 \\ -0.0030 & -0.1023 & 0.0018 \end{pmatrix} \quad (\text{T}/\mu_B) \quad (3)$$

for the Se(2) site are obtained. In addition, as shown above, all components of Knight shift are negative, which is not explained with the dipole interaction solely. Therefore, the hyperfine coupling constant is not mainly determined by the dipole interaction. One possible origin is the core polarization effect induced by p electrons of the Se atoms, which gives a negative Knight shift. Note that the core polarization effect is typically associated with d electrons,³³⁻³⁶⁾ and there are a few examples of the core polarization by p electrons.^{37,38)}

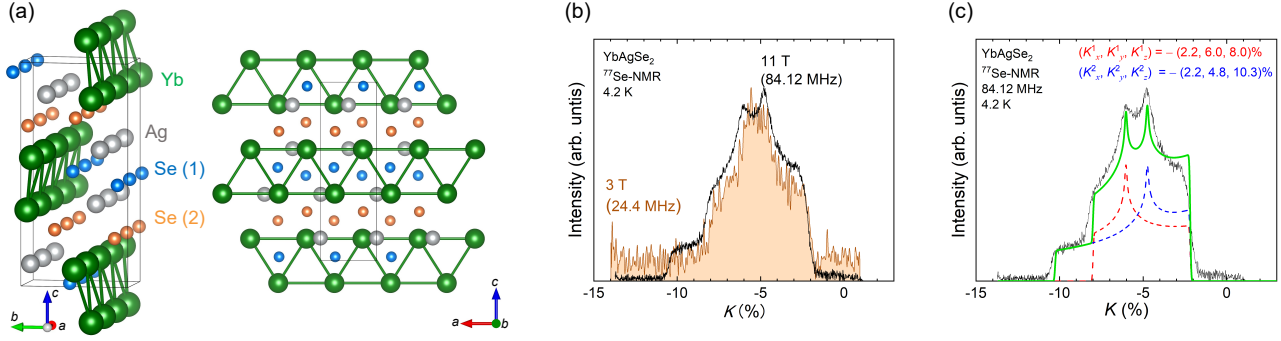


Fig. 1. (Color online) (a) Crystal structure of YbAgSe₂ drawn by VESTA.³¹⁾ (b) The ⁷⁷Se-NMR spectrum obtained by *H*-swept method at 4.2 K at frequencies 24.4 MHz (brown) and 84.12 MHz (black) as a function of ⁷⁷Se-NMR Knight shift. (c) The simulation of the ⁷⁷Se-NMR spectrum with two Se site with Knight shift $(K_x^1, K_y^1, K_z^1) = (-2.2, 6.0, 8.0)\%$ and $(K_x^2, K_y^2, K_z^2) = (2.2, 4.8, 10.3)\%$.

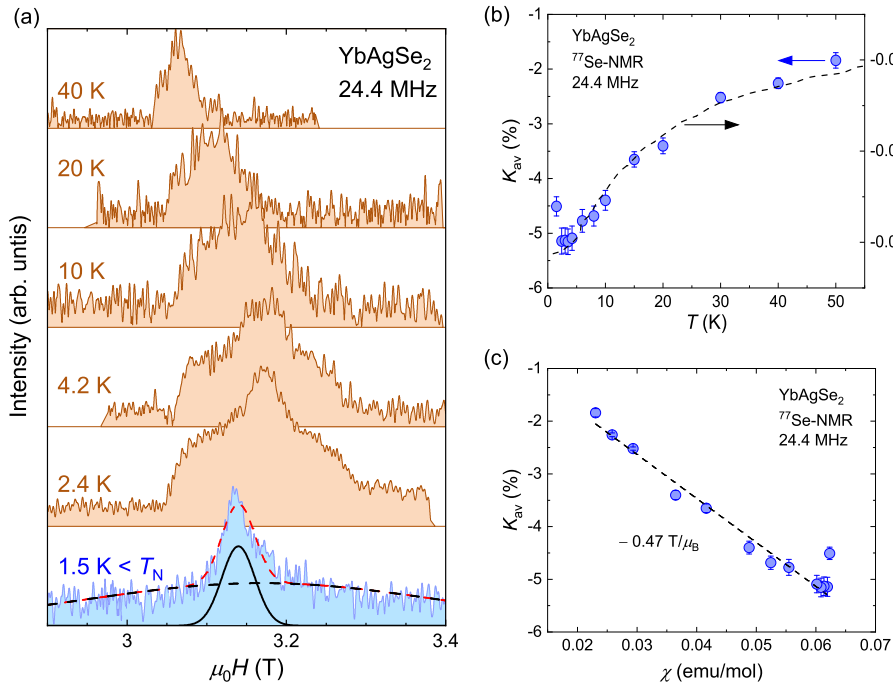


Fig. 2. (Color online) (a) Temperature variations of the ⁷⁷Se-NMR spectrum obtained by *H*-swept method at a frequency of 24.4 MHz for $1.5 \leq T \leq 50$ K. (b) Temperature dependence of the average of ⁷⁷Se-NMR Knight shift K_{av} and bulk magnetic susceptibility χ . (c) K - χ plot with the temperature as an implicit parameter.

Next, we discuss the difference of $1/T_1$ between Yb-zigzag chain systems. Note that the value of $1/T_1 \sim 2000 \text{ s}^{-1}$ at around 4.2 K for YbAgSe₂ is more than one order of magnitude larger than that for YbCuS₂ ($1/T_1 \sim 150 \text{ s}^{-1}$). The difference seems to be consistent with the one in the hyperfine coupling constant. In order to compare the $1/T_1$ behavior of YbCuS₂ and YbAgSe₂, $1/T_1$ was normalized at a value of 4.2 K, and the temperature was normalized with T_N as shown in the inset of Fig. 3. Above T_N , the behavior of $1/T_1$ in YbAgSe₂ is almost the same as that of YbCuS₂ and the critical slowing down behavior was not observed near T_N on both compounds. In previous study,¹²⁾ we reported that the absence

of the critical slowing down behavior is likely to be related to the character of the first-order phase transition in YbCuS₂. However, this contradicts with the experimental result that the specific heat of YbAgSe₂ exhibits a lambda-type anomaly at T_N , indicating a second-order transition.²⁴⁾ Therefore, such a temperature dependence of $1/T_1$ might be a unique behavior on the Yb zigzag chain systems, but the detailed origin remains unclear and further investigations are required.

Below T_N , YbAgSe₂ shows a gapped behavior in $1/T_1$ and T -linear behavior observed in YbCuS₂ was not detected down to 1.0 K. There are three possibilities to explain the absence of the T -linear behavior in YbAgSe₂. One possibility

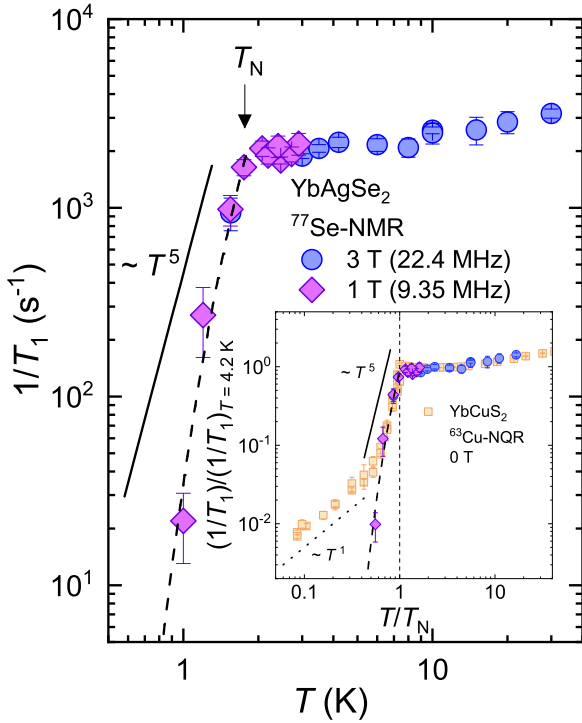


Fig. 3. (Color online) Temperature dependence of the ^{77}Se -NMR nuclear spin-lattice relaxation rates $1/T_1$ in YbAgSe_2 : the circles and diamonds denote $1/T_1$ measured in 3 T (22.4 MHz) and 1 T (9.35 MHz), respectively. The inset shows $(1/T_1)/(1/T_1)_{T=4.2\text{ K}}$ as a function of T/T_N : squares denotes ^{63}Cu -NQR $1/T_1$ measured on YbCuS_2 .¹²⁾

is that the gapless behavior is unique to YbCuS_2 , although both compounds possess the similar Yb zigzag chains. First order character of the magnetic transition might be related to the gapless excitation. Another possibility is that the gapless behavior might be observed at lower temperatures than 1.0 K in YbAgSe_2 . However, the intensity of the ^{77}Se -NMR spectrum in YbAgSe_2 becomes so weak, and T_1 becomes so long below T_N , which give limitations on the temperature range for ^{77}Se -NMR measurements. Currently, NMR measurements can only be performed down to 1.0 K in this compound. The other possibility is that the gapless behavior in YbCuS_2 might be immediately suppressed against magnetic field, because the previous measurements in YbCuS_2 was performed at zero magnetic field. Since Se nuclei have $I = 1/2$, NQR measurements at zero magnetic field are impossible on YbAgSe_2 . Thus, to verify this possibility, ^{63}Cu -NMR $1/T_1$ measurements on YbCuS_2 under magnetic fields or zero-field muon spin resonance in YbAgSe_2 is needed, which is now in progress.

4. Conclusion

In this study, we performed the ^{77}Se -NMR studies on Yb zigzag chain compound YbAgSe_2 to compare to YbCuS_2 . The ^{77}Se -NMR spectrum was fitted by simulating two different Se sites with negative Knight shifts and three-axis anisotropy. The Knight shift is scaled to the bulk magnetic

susceptibility above T_N . Below T_N , the spectral intensity decreases, and the relatively sharp signal and the extremely-broad signal with weak intensity coexist with each other. This observation indicates a difference in the internal fields at the two crystallographically distinct sites below T_N : one site is affected by the internal magnetic fields and the other is not. $1/T_1$ stays almost constant above T_N and follows $1/T_1 \sim \exp(-\Delta/T)$ below T_N , suggesting a magnetic ordered state with magnon gap, but the T -linear behavior of $1/T_1$, which suggests the gapless excitation, was not observed down to 1.0 K. This is in contrast to what was observed in YbCuS_2 , where the T -linear behavior was observed below 0.5 K. It is possible that T -linear behavior is unique to YbCuS_2 , or might be immediately suppressed under the magnetic fields.

The authors would like to thank S. Yonezawa, H. Saito, H. Nakai, and C. Hotta for valuable discussions. This work was supported by Grants-in-Aid for Scientific Research (KAKENHI Grant No. JP20KK0061, No. JP20H00130, No. JP21K18600, No. JP22H04933, No. JP22H01168, No. JP23H01124, No. JP23K22439, No. JP23K25821, No. JP23H04866, No. JP23H04870, No. JP23KJ1247 and No. JP24K00574) from the Japan Society for the Promotion of Science, by JST SPRING (Grant No. JPMJSP2110) from Japan Science and Technology Agency, by research support funding from the Kyoto University Foundation, by ISHIZUE 2024 of Kyoto University Research Development Program, and by Murata Science and Education Foundation. In addition, liquid helium is supplied by the Low Temperature and Materials Sciences Division, Agency for Health, Safety and Environment, Kyoto University.

- 1) Y. Li, H. Liao, Z. Zhang, S. Li, F. Jin, L. Ling, L. Zhang, Y. Zou, L. Pi, Z. Yang, J. Wang, Z. Wu, and Q. Zhang, *Sci. Rep.* **5**, 16419 (2015).
- 2) Y. Li, G. Chen, W. Tong, L. Pi, J. Liu, Z. Yang, X. Wang, and Q. Zhang, *Phys. Rev. Lett.* **115**, 167203 (2015).
- 3) Y. Li, D. Adroja, P. K. Biswas, P. J. Baker, Q. Zhang, J. Liu, A. A. Tsirlin, P. Gegenwart, and Q. Zhang, *Phys. Rev. Lett.* **117**, 097201 (2016).
- 4) K. M. Ranjith, S. Luther, T. Reimann, B. Schmidt, P. Schlender, J. Sichelshmidt, H. Yasuoka, A. M. Strydom, Y. Skourski, J. Wosnitza, H. Kühne, T. Doert, and M. Baenitz, *Phys. Rev. B* **100**, 224417 (2019).
- 5) P.-L. Dai, G. Zhang, Y. Xie, C. Duan, Y. Gao, Z. Zhu, E. Feng, Z. Tao, C.-L. Huang, H. Cao, A. Podlesnyak, G. E. Granroth, M. S. Everett, J. C. Neufeind, D. Voneshen, S. Wang, G. Tan, E. Morosan, X. Wang, H.-Q. Lin, L. Shu, G. Chen, Y. Guo, X. Lu, and P. Dai, *Phys. Rev. X* **11**, 021044 (2021).
- 6) Z. Xiang, Y. Kasahara, T. Asaba, B. Lawson, C. Tinsman, L. Chen, K. Sugimoto, S. Kawaguchi, Y. Sato, G. Li, S. Yao, Y. L. Chen, F. Iga, J. Singleton, Y. Matsuda, and L. Li, *Science* **362**, 65 (2018).
- 7) Y. Sato, Z. Xiang, Y. Kasahara, T. Taniguchi, S. Kasahara, L. Chen, T. Asaba, C. Tinsman, H. Murayama, O. Tanaka, Y. Mizukami, T. Shibauchi, F. Iga, J. Singleton, L. Li, and Y. Matsuda, *Nat. Phys.* **15**, 954 (2019).
- 8) Z. Xiang, L. Chen, K.-W. Chen, C. Tinsman, Y. Sato, T. Asaba, H. Lu, Y. Kasahara, M. Jaime, F. Balakirev, F. Iga, Y. Matsuda, J. Singleton, and L. Li, *Nat. Phys.* **17**, 788 (2021).
- 9) Y. Sato, S. Suetsugu, T. Tominaga, Y. Kasahara, S. Kasahara, T. Kobayashi, S. Kitagawa, K. Ishida, R. Peters, T. Shibauchi, A. H. Nevidomskyy, L. Qian, E. Morosan, and Y. Matsuda, *Nat. Commun.*

- 13, 394 (2022).
- 10) S. Kitagawa, T. Kobayashi, F. Hori, K. Ishida, A. H. Nevidomskyy, L. Qian, and E. Morosan, *Phys. Rev. B* **106**, L100405 (2022).
 - 11) F. Hori, K. Kinjo, S. Kitagawa, K. Ishida, Y. Ohmagari, and T. Onimaru, *J. Phys.: Conf. Ser.* **2164**, 012027 (2022).
 - 12) F. Hori, K. Kinjo, S. Kitagawa, K. Ishida, S. Mizutani, R. Yamamoto, Y. Ohmagari, and T. Onimaru, *Commun. Mater.* **4**, 55 (2023).
 - 13) L. D. Gulay and I. D. Olekseyuk, *J. Alloys Compd.* **402**, 89 (2005).
 - 14) C. K. Majumdar and D. K. Ghosh, *J. Math. Phys.* **10**, 1399 (1969).
 - 15) K. Okunishi and T. Tonegawa, *J. Phys. Soc. Jpn.* **72**, 479 (2003).
 - 16) T. Hikihara, L. Kecke, T. Momoi, and A. Furusaki, *Phys. Rev. B* **78**, 144404 (2008).
 - 17) T. Hikihara, T. Momoi, A. Furusaki, and H. Kawamura, *Phys. Rev. B* **81**, 224433 (2010).
 - 18) H. Saito, H. Nakai, and C. Hotta, *J. Phys. Soc. Jpn.* **93**, 034701 (2024).
 - 19) H. Saito and C. Hotta, *Phys. Rev. Lett.* **132**, 166701 (2024).
 - 20) H. Saito and C. Hotta, *Phys. Rev. B* **110**, 024409 (2024).
 - 21) Y. Ohmagari, Y. Yamane, T. Onimaru, K. Umeo, Y. Shimura, and T. Takabatake, *JPS Conf. Proc.* **30**, 011167 (2020).
 - 22) Y. Ohmagari, T. Onimaru, Y. Yamane, Y. Shimura, K. Umeo, T. Takabatake, H. Sato, N. Kikugawa, T. Terashima, H. T. Hirose, and S. Uji, *J. Phys. Soc. Jpn.* **89**, 093701 (2020).
 - 23) M. Duczmal and S. Pokrzywnicki, *J. Alloys Compd.* **323-324**, 513 (2001).
 - 24) S. Mizutami, Y. Ohmagari, T. Onimaru, Y. Shimura, R. Yamamoto, K. Umeo, and T. Takabatake, *J. Phys.: Conf. Ser.* **2164**, 012025 (2022).
 - 25) S. Mizutami, Y. Ohmagari, T. Onimaru, Y. Shimura, R. Yamamoto, K. Umeo, and T. Takabatake, unpublished.
 - 26) S. Takagi, A. Oyamada, and T. Kasuya, *J. Phys. Soc. Jpn.* **57**, 1456 (1988).
 - 27) K. Ishida, K. Okamoto, Y. Kawasaki, Y. Kitaoka, O. Trovarelli, C. Geibel, and F. Steglich, *Phys. Rev. Lett.* **89**, 107202 (2002).
 - 28) R. Sarkar, R. Gumenuk, A. Leithe-Jasper, W. Schnelle, Y. Grin, C. Geibel, and M. Baenitz, *Phys. Rev. B* **88**, 201101 (2013).
 - 29) S. Tomisawa, T. Mito, S. Wada, K. Hashi, T. Shimizu, A. Goto, S. Ohki, Y. Kato, and M. Kosaka, *J. Phys. Soc. Jpn.* **77**, 291 (2008).
 - 30) M. S. Grbić, E. C. T. O'Farrell, Y. Matsumoto, K. Kuga, M. Brando, R. K uchler, A. H. Nevidomskyy, M. Yoshida, T. Sakakibara, Y. Kono, Y. Shimura, M. L. Sutherland, M. Takigawa, and S. Nakatsuji, *Nat. Commun.* **13**, 2141 (2022).
 - 31) K. Momma and F. Izumi, *J. Appl. Crystallogr.* **44**, 1272 (2011).
 - 32) F. Hori, S. Kitagawa, K. Ishida, Y. Ohmagari and T. Onimaru, unpublished.
 - 33) A. M. Clogston, V. Jaccarino, and Y. Yafet, *Phys. Rev.* **134**, A650 (1964).
 - 34) H. T. Weaver and R. K. Quinn, *Phys. Rev. B* **10**, 1816 (1974).
 - 35) K. Ishida, Y. Kitaoka, K. Asayama, S. Ikeda, S. Nishizaki, Y. Maeno, K. Yoshida, and T. Fujita, *Phys. Rev. B* **56**, R505(R) (1997).
 - 36) R. Ray, A. Ghoshray, K. Ghoshray, and S. Nakamura, *Phys. Rev. B* **59**, 9454 (1999).
 - 37) K. Magishi, R. Watanabe, A. Hisada, T. Saito, K. Koyama, and T. Fujiwara, *J. Phys. Conf. Ser.* **592**, 012031 (2015).
 - 38) N. Higa, M. Yogi, H. Kuroshima, T. Toji, H. Niki, Y. Hiranaka, A. Nakamura, T. Nakama, M. Hedo, and Y. Ōnuki, *J. Phys. Soc. Jpn.* **87**, 094708 (2018).